Volume 1 | Number 1 | Jan 2013 | Pages 1–100

ChemComm

Chemical Communications
www.rsc.org/chemcomm

ROYAL SOCIETY OF CHEMISTRY

ROYAL SOCIETY OF CHEMISTRY

www.rsc.org/chemcomm

Chemical Communications

COMMUNICATION

SnO₂ nanocrystals anchoring on N-doped graphene for high-performance lithium storage

Wei Zhou[a], Jinxian Wang[a,b], Feifei Zhang[a,c], Shumin Liu[a], Jianwei Wang[a], Dongming Yin[a] and Limin Wang[a,d,*]

SnO₂/N-doped graphene (SnO₂-NG) composite is synthesized by a rapid, facile, one-step microwave-assisted solvothermal method. The composite exhibits excellent lithium storage capability and high durability, and is a promising anode material for lithium ion battery.

Lithium ion batteries are now dominant power sources for portable electronic devices due to high energy density and long cycle life. However, the commercial used carbon anode materials (theoretical specific capacity of 372 mA h g⁻¹) can't meet the increasing demands of critical applications, such as electric vehicles and smart grids. Therefore, it is urgent to develop new high energy capacity anode materials. Tin oxide (SnO_2) has been regarded as a promising anode material, with advantages such as high theoretical specific capacity (782 mA h g⁻¹), low cost and environmental friendliness.[1-7] However, SnO_2 as a semiconductor possesses low conductivity. Furthermore, SnO_2 suffers huge volume change ~300% during charge/discharge cycling leading to pulverization and detachment with the current collector, which results in capacity decay and poor rate performance.[8,9]

To circumvent the above problems, an effective way is to synthesize composite with graphene. N-doped graphene not only inherit the merits of graphene, such as large surface area, exceptional physical and chemical properties, but also obtain tailored properties and broadened applications, such as catalysis and energy storage.[10-15] SnO_2/graphene composite is usually synthesized by mechanical mixing, solvothermal and hydrothermal methods, etc.[16-19] Recently, Guo *et al.* synthesized SnO_2/N-doped graphene hybrid by mixing SnO_2 nanocrystals with graphene oxide (GO) and subsequent hydrazine monohydrate vapor reduction.[20] However, there are few reports about using microwave-assisted solvothermal method. Comparing with convenient hydrothermal/solvothermal method,

microwave-assisted method is more effective in time and energy saving, facile composition and size control, etc.[21-25]

Herein, we designed a rapid, facile microwave-assisted solvothermal method for synthesis SnO_2/N-doped graphene composite, which presented several advantages: (a) the process was one-pot, took only a few minutes and needed no further treatment; (b) fast Li-ion diffusion was obtained due to the small size of SnO_2 nanocrystals; (c) N-doped graphene not only provided fast electron and ion transfer channel, but suppressed the aggregation of SnO_2 during cycling. The electrochemical properties of the composite as anode material were tested by galvanostatic charge/discharge cycling. The results indicated that the composite possessed both good cycling property and high-rate capacity. The superior performances were attributed to the synergistic effect from both components.

During the synthesis process, Sn^{4+} ions were firstly anchored on graphene oxide due to electrostatic attraction. Later, urea was decomposed to release ammonia, which promoted the synthesis of $Sn(OH)_4$ and acted as N source for doping in graphene. Ethylene glycol (EG) was adopted as reducing agent for GO.[26-28] This procedure provided a time and energy saving method for synthesis N-doped graphene-metal oxide composite.

In the XRD patterns (Fig. S1) of SnO_2 nanocrystals and SnO_2-NG composite, the broaden peaks for both can be indexed to tetragonal SnO_2 (JCPDS 41-1445) and indicate the small size of SnO_2 nanocrystals. As for SnO_2-NG composite, the (002) peak of graphene has not been observed, which may due to the relatively weak intensity and overlapping with the (110) peak of SnO_2. As shown in Fig. S2, tiny SnO_2 nanocrystals are loosely assembled in graphene free sample. In contrast, SnO_2 nanocrystals are densely anchored on graphene nanosheets in SnO_2-NG composite (Fig. 1). The HRTEM image (Fig. 1b) displays that the SnO_2 nanocrystals are with an average size about 3 nm and the 0.33 nm lattice fringes are corresponding to the (110) planes of tetragonal SnO_2. The TGA

curve (Fig. S3) indicates that the content of SnO_2 in the composite is around 75 wt%. Additionally, elemental mapping images (Fig. S4) reveal that N, C and Sn elements are uniformly dispersed in the composite.
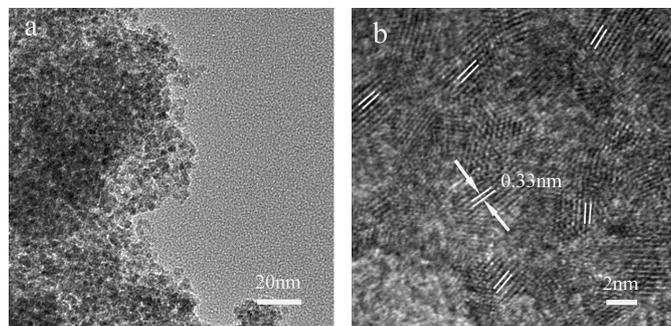
Fig.1 TEM (a) and HRTEM (b) images of SnO_2/N-doped graphene composite.

The reducing process of GO and formation of N-doped graphene are further investigated by X-ray photoelectron spectroscopy (XPS). The C1s XPS spectra (Fig. S5) manifest three peaks corresponding to C-C bond (284.6 eV) of sp^2 carbon, C-O (~286.6 eV) and C=O (~288.7 eV) bonds, respectively.[29] The peak intensities of C-O and C=O bonds are greatly reduced and the C-C bond content is increased after the solvothermal reaction. Furthermore, C-N bond (~286.0 eV) is introduced after N doping.[30]

N、C and Sn elements are obviously seen in the XPS spectrum (Fig. 2a). The pressure produced in the solvothermal process has a promotive effect on reduction and N-doping of GO.[31] However, N element is not found in the XPS spectrum of SnO_2-graphene hybrid synthesized by microwave refluxing at 90 °C.[32] Therefore it may be concluded that temperature and pressure are vital for N doping in graphene. The deconvoluted N 1s spectrum (Fig. 2b) is fitted by two main peaks at 398.3 eV and 399.4 eV, respectively, and which correspond to pyridinic N and pyrrolic N.[31,33] Based on the XPS result, the atomic ratio of N element is 1.2% and the ratio between pyridinic N and pyrrolic N is 70%. It was reported that the pyridinic-like structure can provide a feasible pathway for Li ion penetration.[34] N-doped graphene are beneficial for transportation of both electron and Li ion. Therefore good rate performance can be expected for the composite.
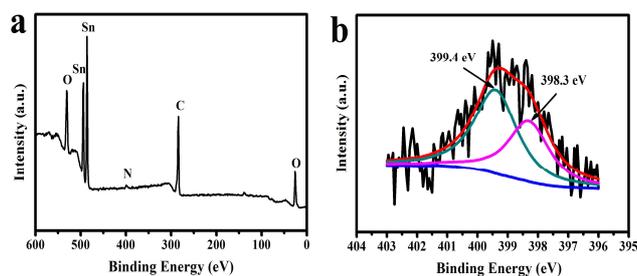
Fig.2 The XPS (a) and deconvoluted N 1s (b) curves of SnO_2/N-doped graphene composite.

The electrochemical properties of SnO_2 nanocrystals and SnO_2-NG composite are characterized by galvanostatic discharge/charge measurements at various C rates. Considering the theoretical specific capacities of SnO_2 and graphene (782 mA h g^{-1} and 744 mA h g^{-1}) are close, here 1 C denotes as 782 mA h g^{-1}. The cycle performances of SnO_2 nanocrystals and SnO_2-NG composite at 1 C rate are shown in Fig. 3a. The cells are firstly discharge/charge 10 cycles at 0.3 C. For SnO_2 nanocrystals, the first discharge capacity reaches 1233 mA h g^{-1}. However, the capacity shows continuous decay along with cycle processing and only retains 65 mA h g^{-1} after 270th cycle at 1 C rate. This feature is common for pristine SnO_2 nanocrystals, due to the pulverization and detaching contact with current collector as mentioned above. In contrast, the initial discharge capacity of SnO_2-NG is much higher and reaches 1807 mA h g^{-1}. In the 1st cycle at 1 C rate, the capacity reaches 999 mA h g^{-1} and retains 853 mA h g^{-1} after 270th cycle at 1 C. The capacity is higher than the theoretical specific capacities of SnO_2 and graphene. This may be resulted from the extra lithium storage capacity provided by polymeric gel-like films.[35-37]

The typical charge/discharge curves of SnO_2-NG composite at various C rates are illustrated in Fig. 3b. The discharge capacities reach 1123, 969, 818, 580 and 369 mA h g^{-1}, when current rates are 0.3 C, 1 C, 2 C, 5 C and 10 C, respectively. Even at 10 C rate, the capacity is still comparable with the theoretical capacity of graphite.

As shown in Fig. 3c, the rate performance of pristine SnO_2 nanocrystals is relatively poor. The capacity reaches only about 20 mA h g^{-1} at 10 C rate. Though it increases to 448 mA h g^{-1} when current rate reverts to 0.3 C, a fast decay is obvious and the capacity retains only 85 mA h g^{-1} after 170 cycles at 0.3 C. In contrast, SnO_2-NG composite shows much better rate performance (Fig. 3d). After 10 cycles at 10 C, the capacity reverts to 981 mA h g^{-1} and retains 937 mA h g^{-1} after 170 cycles at 0.3 C. The capacity retention reaches 96%, which is much higher than that of SnO_2 nanocrystals.
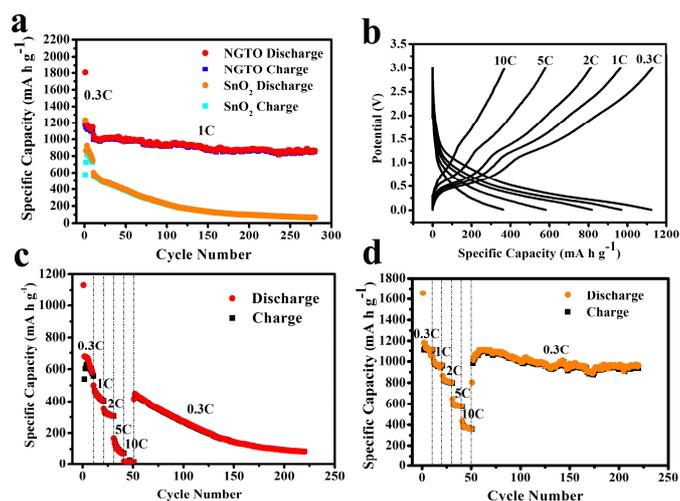
Fig.3 (a) Cycle performance of SnO_2 nanocrystals and SnO_2-NG electrodes at 1 C; (b) Typical charge-discharge curves of SnO_2-NG electrode at various C rates; rate performance of (c) SnO_2 nanocrystals and (d) SnO_2-NG electrodes at various current densities from 0.3 to 10 C with respect to the cycle numbers.

The structure of SnO_2-NG electrode after 270th cycle at 1 C is shown in Fig. S6. Tiny nanocrystals still densely anchor on graphene as before and no aggregation appears. In HRTEM, the lattice fringe of 0.36 nm is corresponding to the (220) planes of Li_2Sn_5 (JCPDS 74-0561). Therefore it can be concluded that the composite has good structure stability and thus superior cycling stability is achieved.

In summary, superior electrochemical properties are realized from SnO_2-NG composite synthesized by microwave-assisted solvothermal method. The high-performance lithium storage properties are due to the synergistic effect from both SnO_2 nanocrystals and N-doped graphene. SnO_2-NG composite is a promising anode material, and the procedure used here may provide a time and energy saving method for synthesizing other N-doped graphene-metal oxide composite.

Notes and references

^{a} State Key Laboratory of Rare Earth Resource Utilization, Changchun Institute of Applied Chemistry, Chinese Academy of Sciences, Changchun 130022, China.

^{b} School of Chemistry and Environmental Engineering, Changchun University of Science and Technology, Changchun 130022, China.

^{c} University of Chinese Academy of Sciences, Beijing 100049, China.

^{d} Changzhou Institute of Energy Storage Materials and Devices, Changzhou, 213000, China.

* Corresponding author. Tel.: +86 431 85262447. Fax: +86 431 85262836. E-mail address: lmwang@ciac.ac.cn

1 J.S. Chen and X.W. Lou, *Small*, 2013, **9**, 1877.
2 L.-Y. Jiang, X.-L. Wu, Y.-G. Guo and L.-J. Wan, *J. Phys. Chem. C*, 2009, **113**, 14213.
3 L.M. Li, X.M. Yin, S. Liu, Y.G. Wang, L.B. Chen and T.H. Wang, *Electrochem. Commun.*, 2010, **12**, 1383.
4 S.J. Ding, D.Y. Luan, F.Y.C. Boey, J.S. Chen and X.W. Lou, *Chem. Commun.*, 2011, **47**, 7155.
5 Y.-D. Ko, J.-G. Kang, J.-G. Park, S. Lee and D.-W. Kim, *Nanotechnology*, 2009, **20**, 455701.
6 Y.M. Li, X.J. Lv, J. Lu and J.H. Li, *J. Phys. Chem. C*, 2010, **114**, 21770.
7 K. Shiva, H.B. Rajendra, K.S. Subrahmanyam, A.J. Bhattacharyya and C.N.R. Rao, *Chem. Eur. J.*, 2012, **18**, 4489.
8 D. Deng, M.G. Kim, J.Y. Lee and J. Cho, *Energy Environ. Sci.*, 2009, **2**, 818.
9 J.-H. Kang, S.-M. Paek and J.-H. Choy, *Chem. Commun.*, 2012, **48**, 458.
10 B. You, L.L. Wang, L. Yao and J. Yang, *Chem. Commun.*, 2013, **49**, 5016.
11 C.Y. He, R.H. Wang, H.G. Fu and P.K. Shen, *J. Mater. Chem. A*, 2013, **1**, 14586.
12 S.B. Yang, L.J. Zhi, K. Tang, X.L. Feng, J. Maier and K. Müllen, *Adv. Funct. Mater.*, 2012, **22**, 3634.
13 H.Q. Sun, Y.X. Wang, S.Z. Liu, L. Ge, L. Wang, Z.H. Zhu and S.B. Wang, *Chem. Commun.*, 2013, **49**, 9914.
14 B.D. Guo, Q. Liu, E.D. Chen, H.W. Zhu, L. Fang, and J.R. Gong, *Nano Lett.*, 2010, **10**, 4975.
15 J.L. Zhu, C.Y. He, Y.Y. Li, S. Kang and P.K. Shen, *J. Mater. Chem. A*, 2013, **1**, 14700.
16 S.-M. Paek, E. Yoo and I. Honma, *Nano Lett.*, 2009, **9**, 72.
17 D.N. Wang, X.F. Li, J.J. Wang, J.L. Yang, D.S. Geng, R.Y. Li, M. Cai, T.-K. Sham and X.L. Sun, *J. Phys. Chem. C*, 2012, **116**, 22149.
18 H.W. Song, N. Li, H. Cui and C.X. Wang, *J. Mater. Chem. A*, 2013, **1**, 7558.
19 J.X. Guo, B. Jiang, X. Zhang, H.T. Liu, *J. Power Sources*, 2014, **262**, 15.
20 X.S. Zhou, L.-J. Wan and Y.-G. Guo, *Adv. Mater.*, 2013, **25**, 2152.
21 F. Yu, S.H. Lim, Y.D. Zhen, Y.X. An and J.Y. Lin, *J. Power Sources*, 2014, **271**, 223.
22 S.Q. Chen, Y. Wang, H. Ahn and G.X. Wang, *J. Power Sources*, 2012, **216**, 22.
23 C.-L. Liu, K.-H. Chang, C.-C.Hu and W.-C. Wen, *J. Power Sources*, 2012, **217**, 184.
24 F. Yu, L.L. Zhang, M.Y. Zhu, Y.X. An, L.L. Xia, X.G. Wang and B. Dai, *Nano Energy*, 2014, **3**, 64.
25 L.Q. Lu and Y. Wang, *J. Mater. Chem.*, 2011, **21**, 17916.
26 Y. Chen, B.H. Song, X.S. Tang, L. Lu and J.M. Xue, *J. Mater. Chem.*, 2012, **22**, 17656.
27 L. Ye, J.L. Fu, Z. Xu, R.S. Yuan and Z.H. Li, *ACS Appl. Mater. Interfaces*, 2014, **6**, 3483.
28 X.F. Lu , L. Yang , X.J. Bian , D.M. Chao and C. Wang, *Part. Part. Syst. Charact.*, 2014, **31**, 245.
29 S. Yang , W.B. Yue , J. Zhu , Y. Ren , and X.J. Yang, *Adv. Funct. Mater.*, 2013, **23**, 3570.
30 S. Indrawirawan, H.Q. Sun, X.G. Duan and S.B. Wang, *J. Mater. Chem. A*, 2014, DOI: 10.1039/C4TA05940A.
31 G. Wang, L.-T. Jia, Y. Zhu, B. Hou, D.-B. Li and Y.-H. Sun, *RSC Adv.*, 2012, **2**, 11249.
32 Y.Q. Zhu, C. Li and C.B. Cao, *RSC Adv.*, 2013, **3**, 11860.
33 F. Zou, X.L. Hu, Y.M. Sun, W. Luo, F.F. Xia, L. Qie, Y. Jiang and Y.H. Huang, *Chem. Eur. J.*, 2013, **19**, 6027.
34 Y.F. Li, Z. Zhou, L.B. Wang, *J. Chem. Phys.*, 2008, **129**, 104703.
35 S. Laruelle, S. Grugeon, P. Poizot, M. Dolle, L. Dupont, and J-M. Tarascon, *J. Electrochem. Soc.*, 2002, **149**, A627.
36 G. Gao, S. Lu, B. Dong, Z. Zhang, Y. Zheng and S. Ding, *J. Mater. Chem. A*, 2014, DOI: 10.1039/C4TA05725B.
37 B. Liu, J. Zhang, X.F. Wang, G. Chen, D. Chen, C.W. Zhou, and G.Z. Shen, *Nano Lett.*, 2012, **12**, 3005.

ChemComm Accepted Manuscript